Title

Role of Reynolds stress and toroidal momentum transport in the dynamics of internal transport barriers

Journal

Physics of Plasmas, 19(8)

ISSN

1070-664X

Authors

Kim, SS
Jhang, Hogun
Diamond, PH

Publication Date

2012-08-01

DOI

10.1063/1.4743024

Role of Reynolds stress and toroidal momentum transport in the dynamics of internal transport barriers

S. S. Kim,[a] Hogun Jhang, and P. H. Diamond[b]
WCI Center for Fusion Theory, National Fusion Research Institute, Daejon, South Korea

(Received 29 February 2012; accepted 25 July 2012; published online 8 August 2012)

We study the interplay between intrinsic rotation and internal transport barrier (ITB) dynamics through the dynamic change of the parallel Reynolds stress. Global flux-driven gyrofluid simulations are used for this study. In particular, we investigate the role of parallel velocity gradient instability (PVGI) in the ITB formation and the back transition. It is found that the excitation of PVGI is followed by a change in the Reynolds stress which drives a momentum redistribution. This significantly influences $E \times B$ shear evolution and subsequent ITB dynamics. Nonlocal interactions among fluctuations are also observed during the PVGI excitation, resulting in turbulence suppression at the ITB. © *2012 American Institute of Physics*. [http://dx.doi.org/10.1063/1.4743024]

There is a growing interest in the effect of toroidal rotation on plasma confinement. Experimental results indicate that confinement degrades as rotation drops[1–3] and that high rotational shear mitigates T_i profile stiffness at low magnetic shear.[4] Theoretical works have shown that turbulence can be fully quenched by flow shear at zero magnetic shear,[5] and external torque can trigger or facilitate a transport bifurcation.[5,6] Although counter examples exist (e.g., Ref. 7), these results imply that rotation and rotational shear might be advantageous to enhanced confinement. The role of intrinsic rotation in enhancing confinement is also of great interest, due to the limited capability for momentum injection in reactor-scale experiments.[8] It is likely that intrinsic rotation, which is generated by conversion of radial inhomogeneity into $k_{||}$ asymmetry via residual stress,[9,10] is strongly coupled to transport barrier evolution. Intrinsic rotation can also affect transport barrier formation by driving a strong mean $E \times B$ shear, thus suggesting a possible feedback loop which enhances the internal transport barrier (ITB). Recent experiments at Alcator C-Mod (Ref. 11) have shown that the $E \times B$ shearing rate closely tracks the contribution from the parallel flow gradient ($\nabla V_{||}$). A recent gyrofluid simulation study demonstrated the coupling of intrinsic rotation to ITB dynamics.[12]

In this paper, we study the interplay between intrinsic rotation and barrier dynamics mediated by Reynolds stress and $\nabla V_{||}$-dominated $E \times B$ shear. This work was motivated by an interesting observation made in Ref. 12, where we observed that the parallel Reynolds stress changes significantly before and during ITB formation and back transition. The primary objectives of this paper are to identify a possible hidden dynamical process which underlies this phenomenon and to elucidate its role in ITB dynamics. In particular, we focus on the onset of parallel velocity gradient instability (PVGI) during barrier evolution. The PVGI is a negative compressibility mode driven by $\nabla V_{||}$ and ∇T_i.[13–15] Numerical studies demonstrated that PVGI can be excited at high $|\nabla V_{||}|$ (Ref. 16) and affect ITB.[17] Figure 1 shows the interplay between Reynolds stress ($\langle \tilde{V}_r \tilde{V}_{||} \rangle$), intrinsic rotation, $E \times B$ shear, and T_i profile via PVGI during ITB formation. The onset of PVGI relaxes $\nabla V_{||}$ by enhancing the diffusive part of the Reynolds stress.[14] The Reynolds stress controls the radial profile of intrinsic rotation and receives feedback from $\nabla V_{||}$, through PVGI and its induced diffusive flux. The key point is that a feedback process (involving PVGI) between Reynolds stress and $\nabla V_{||}$ can increase $|\nabla V_{||}|$ at the ITB position. Since $E \times B$ shear is governed not only by $\nabla^2 T_i$ but also by $\nabla V_{||}$, this process may trigger ITB formation. The other subject that we will address in this paper is nonlocal interaction among fluctuations. Itoh *et al.* pointed out that stronger fluctuations at a certain position can suppress weaker fluctuations at neighboring locations via inducing zonal flows.[18] The range of this interaction is mesoscale, i.e., characteristic of the zonal flow ($\sim\sqrt{\rho_i L}$). In this case, the PVGI could strengthen an ITB (i.e., reduce fluctuations at the ITB position) if the most unstable position is located near the ITB position (but not at the ITB position).

We make a detailed analysis of a long time power ramp simulation as shown in Fig. 2(a), which was reported in Ref. 12 by using a modified version of the TRB code.[19] In TRB, electrostatic ion turbulence is studied using a three-field model.[19] The TRB code was used in studying the role of magnetic shear in ITB formation[19] and the effect of sheared flow on ITB (Ref. 17) at fixed powers. In this simulation, a heat source is ramped up and down at a sufficiently slow rate.[20] A reversed q profile and a no-slip boundary condition on $V_{||}$ are used, and no external torque is applied. Only resonant modes, which are radially localized around rational surfaces, are retained for fluctuating quantities. This is a major limitation of our numerical model. The importance of nonresonant modes near the $q' = 0$ region, where barrier formation occurs, was pointed out in Ref. 21. We note, though that the physics behind the role of nonresonant modes in ITB formation and back transition has not been fully understood. We give a brief discussion of the reliability of our results at the end of this paper. Density and electron temperature

[a]Electronic mail: sskim@nfri.re.kr.
[b]Also at Center for Astrophysics and Space Sciences and Department of Physics, University of California San Diego, La Jolla, California 92093-0429, USA.

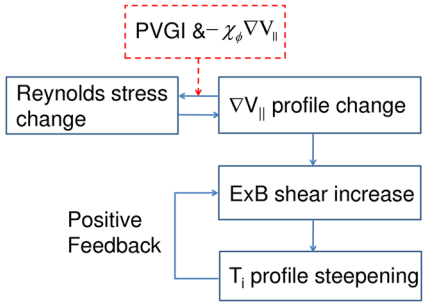

FIG. 1. A schematic diagram showing the interplay between Reynolds stress, intrinsic rotation, $E \times B$ shear, and T_i profile during ITB formation. Reynolds stress gets feedback from $\nabla V_{||}$ through PVGI and its induced diffusive flux ($-\chi_\phi \nabla V_{||}$).

profiles are fixed during the simulation. Adiabatic electrons and flat density profile are assumed, which are other limitations of this study, as compared with experiments, where a peaked density profile is usually observed in an ITB.[8,11] We also mention that an external torque is necessary for ion ITB formation in real experiments.[1,2] Thus, our numerical results are still far from explaining experimental observations, due to these limitations of the simulation model. In Fig. 2(a), a sudden increase or decrease of $|\nabla T_i|$ is accompanied by a decrease or increase of the turbulent heat flux which implies ITB formation and back transition. Figure 2(a) indicates that $|\nabla T_i|/T_i$ are positively correlated with rotational shear, which is consistent with ion stiffness mitigation experiments at high rotational shear and low magnetic shear in JET.[4] Figure 2(b) shows typical T_i and $V_{||}$ profiles after ITB formation. Several positions that are expected to be important are designated by the labels r_1, r_2, r_3, r_4 in Fig. 2(b). r_1 is the location of maximal $|\nabla V_{||}|$ (i.e., PVGI driver), and r_4 corresponds to the position where PVGI is distinct. r_2 is the location of q_{min} (minimal q), where dynamic change of ITB occurs. We found that a large fluctuation due to PVGI at $r = r_4$ induces zonal flow formation at neighboring location, i.e., $r = r_3$.

In Fig. 3, we investigate the onset of PVGI during ITB evolution. Figure 3(a) shows the time histories of $\nabla V_{||}$ and

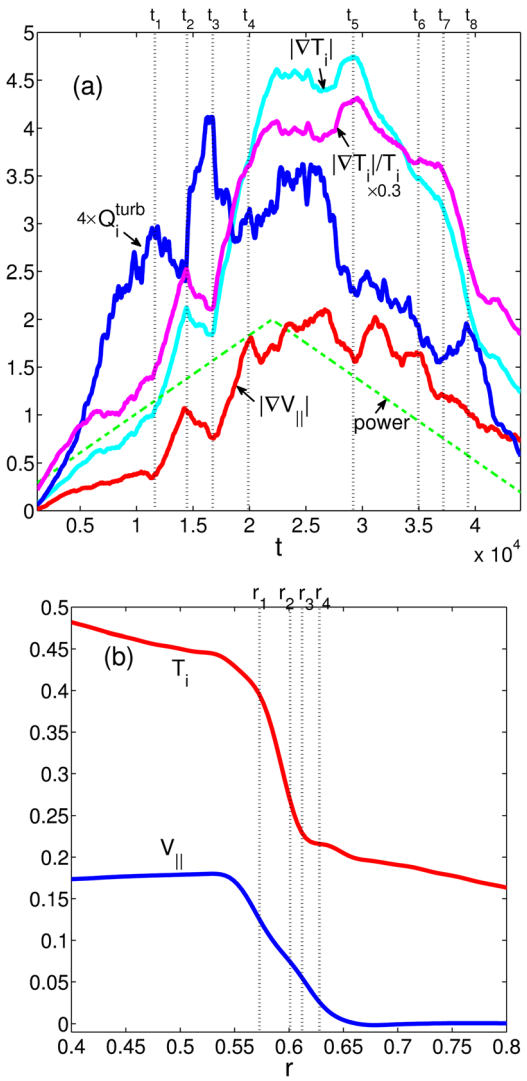

FIG. 2. (a) Time histories of turbulent heat flux Q_i^{turb}, $|\nabla T_i|$, $|\nabla T_i|/T_i$ and $|\nabla V_{||}|$ at ITB in power ramp simulation.[12] $t_{1\sim8}$ represent transition or instability peak points. (b) Profiles of T_i and $V_{||}$ after ITB formation (at $t = t_5$). Same normalizations as Ref. 12 are used in this paper.

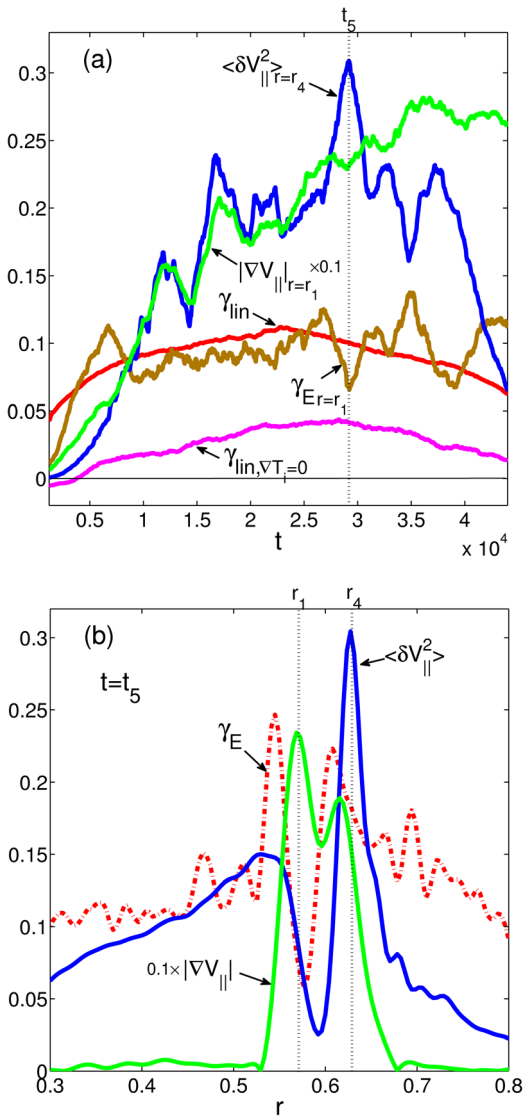

FIG. 3. (a) Time histories of $|\nabla V_{||}|$ and $E \times B$ shearing rate γ_E at $r = r_1$, $\langle \delta V_{||}^2 \rangle$ at $r = r_4$, and linear growth rate γ_{lin} during power ramps. $\gamma_{lin,\nabla T_i=0}$ is linear growth rate for $\nabla T_i = 0$. (b) Radial profiles of $\langle \delta V_{||}^2 \rangle$, $|\nabla V_{||}|$, and γ_E at $t = t_5$.

the $E \times B$ shearing rate γ_E at $r = r_1$ during power ramps. They are compared to parallel flow fluctuation intensity $\langle \delta V_{||}^2 \rangle$ at $r = r_4$ and global linear growth rate γ_{lin} computed by using T_i and $V_{||}$ profiles in the simulation. To ensure that the linear mode grows by parallel shear flow, we also calculated the growth rate ($\gamma_{lin,\nabla T_i=0}$) in the absence of ∇T_i and compared it with γ_{lin}, as shown in Fig. 3(a). During the initial phase when intrinsic rotation is not sufficiently developed, $\gamma_{lin,\nabla T_i=0}$ has negative values while it becomes positive (i.e., unstable) and increases with increasing $|\nabla V_{||}|$ later on. Since the only remaining free energy source in this case is $\nabla V_{||}$, the growing mode can be unambiguously identified as the PVGI. In the present numerical model, only the tails of the modes can penetrate into the ITB region, due to the lack of resonant modes near the q_{min} region. The fluctuations which penetrate are affected by the strong ∇T_i and $\nabla V_{||}$. The effects of strong gradients on the unstable mode in this region may be underestimated because of the absence of nonresonant modes. In Fig. 3(a), one can observe several peaks in $\langle \delta V_{||}^2 \rangle$ at $r = r_4$ when γ_E at $r = r_1$ is smaller than γ_{lin}, implying the onset of PVGI. We plot the radial profile of $\langle \delta V_{||}^2 \rangle$ in Fig. 3(b) together with $\nabla V_{||}$ (i.e., the PVGI driver) and γ_E when PVGI is markedly excited (i.e., at $t = t_5$). Since $r = r_1$ is co-located with the ITB shoulder, contributions of $\nabla V_{||}$ and $\nabla^2 T_i$ to the total $E \times B$ shear nearly cancel each other and γ_E has a local minimum at this position. It seems that due to strong $E \times B$ shearing—a well known turbulence suppressor[22,23]—the most unstable position appears to be outside the ITB (i.e., at $r = r_4$).

In Fig. 4, we explore momentum transport due to PVGI and its impact on ITB dynamics. Figure 4(a) compares time evolution of Reynolds stress $\Pi_{r||}$ at $r = r_1$ and $\nabla V_{||}$, γ_E, zonal flow shear γ_{ZF} at $r = r_2$, with $\langle \delta V_{||}^2 \rangle$ at $r = r_4$. We notice that onset of PVGI is followed by a change of Reynolds stress during forward transition. This drives a momentum redistribution which significantly affects $\nabla V_{||}$ at q_{min} position ($r = r_2$). Since γ_E closely tracks $\nabla V_{||}$ at $r = r_2$ as shown in Fig. 4(a), this PVGI-induced change of $\nabla V_{||}$ at $r = r_2$ plays a significant role in ITB formation. We note that both the usual positive feedback between γ_E and T_i profile steepening and the momentum redistribution due to PVGI accelerate the increase of γ_E during the forward transition. A comparison of γ_E with γ_{ZF} shows that the forward transition occurs when the mean shear flow develops with increasing $V_{||}$ gradient. Figure 4(b) shows the profile evolution of $\nabla V_{||}$ during the ITB formation period ($t_1 \le t \le t_4$). During burst-like changes in $\Pi_{r||}$ after PVGI at $t = t_1$ and t_3, the radial profile of $\nabla V_{||}$ relaxes from bimodal to unimodal one, and the forward transition occurs.

Figure 5 presents an interesting observation, where time histories of $E \times B$ shear at $r = r_2$ and $|\nabla T_i|$ at the ITB are plotted during the ITB persistence time. One finds that once formed, the ITB is robust, regardless of the dynamic change of γ_E. Around $t = t_5$, the ITB becomes rather strong in spite of γ_E reduction, as can be seen by the green line in Fig. 5. To understand this seemingly contradictory result, we also plot the T_i fluctuation intensity $\langle \delta T_i^2 \rangle$ at $r = r_2$ and compare it to $\langle \delta V_{||}^2 \rangle$ at $r = r_4$ and γ_{ZF} at $r = r_3$. The reduction of $\langle \delta T_i^2 \rangle$ around $t = t_5$ implies that the confinement enhancement is due to turbulence suppression. One can observe from Fig. 5

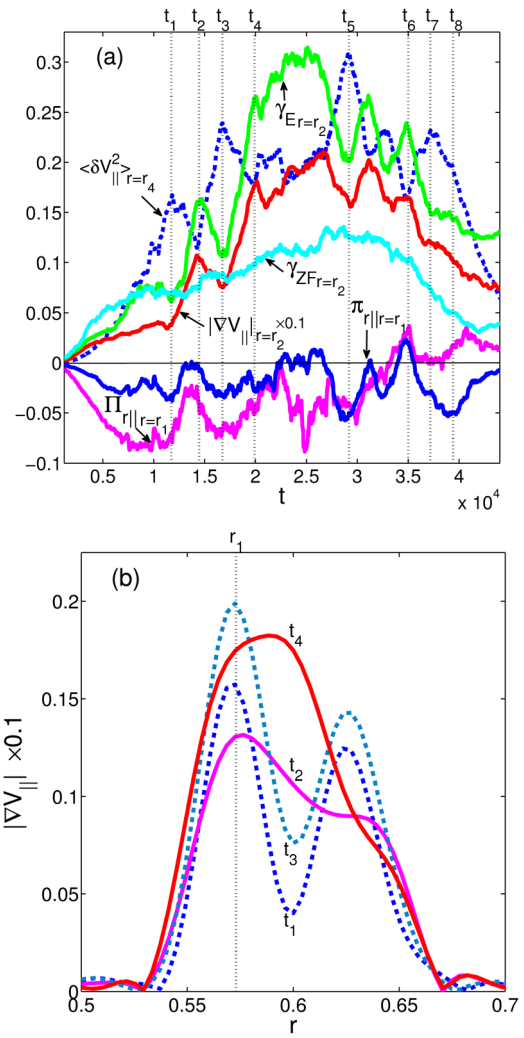

FIG. 4. (a) Time histories of parallel Reynolds stress $\Pi_{r||}$ at $r = r_1$, γ_E, zonal flow shear γ_{ZF}, $|\nabla V_{||}|$ at $r = r_2$, and $\langle \delta V_{||}^2 \rangle$ at $r = r_4$ during power ramps. $\pi_{r||}$ means contribution of resonant modes with $m/n = 49/32$ and $74/48$ to $\Pi_{r||}$. (b) Profile evolution of $|\nabla V_{||}|$ during forward transition period ($t_1 \le t \le t_4$).

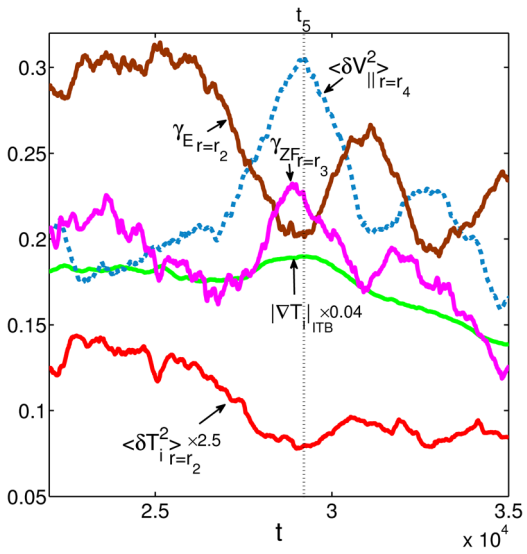

FIG. 5. Time histories of γ_E, $\langle \delta T_i^2 \rangle$ at $r = r_2$, $|\nabla T_i|$ averaged within ITB, γ_{ZF} at $r = r_3$, and $\langle \delta V_{||}^2 \rangle$ at $r = r_4$ during the ITB sustainment phase.

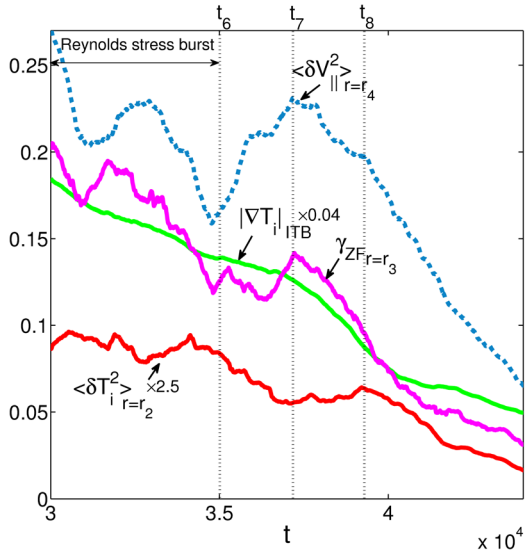

FIG. 6. Time histories of $\langle \delta T_i^2 \rangle$ at $r = r_2$, γ_{ZF} at $r = r_3$, $\langle \delta V_{||}^2 \rangle$ at $r = r_4$, and $|\nabla T_i|$ at ITB, from Reynolds stress burst period to final ramp-down.

that the excitation of PVGI (at $t = t_5$) causes the growth of γ_{ZF} at $r = r_3$, resulting in the reduction of $\langle \delta T_i^2 \rangle$ at $r = r_2$. A possible interpretation of this result is that stronger fluctuations at the unstable position ($r = r_4$) suppress weaker fluctuations at the nearby position ($r = r_2$), via zonal flow induction at a location between them ($r = r_3$). A similar dynamical mechanism was proposed by Itoh *et al.*[18]

In Ref. 12, we found that an outward momentum transfer is caused by Reynolds stress burst prior to back transition and leads to barrier destruction.[12] Here, we address the back transition process and focus on the effect of the PVGI. In Fig. 4(a), the link between $\Pi_{r||}$ and PVGI is not straightforward, for times after the forward transition. To see this note that the Reynolds stress can be represented as a sum of contributions from resonant modes. Contributions from resonant modes with $m/n = 49/32$ and $74/48$ dominate $\Pi_{r||}$ at $r = r_1$ during the Reynolds stress burst prior to the back transition. In Fig. 4(a), their sum $\pi_{r||}$ is plotted. One can see that the dominant mode contribution follows $\langle \delta V_{||}^2 \rangle$ more systematically after the ITB formation. This supports the hypothesis that PVGI onset at $t = t_5$ is responsible for the Reynolds stress burst which triggers the back transition. Figure 6 shows T_i and $V_{||}$ fluctuation intensities at $r = r_2$ and r_4, together with the $|\nabla T_i|$ of the ITB and γ_{ZF} at $r = r_3$, during the back transition. One can see that PVGI is excited in the back transition phase (at $t = t_7$). Comparing Fig. 6 with Fig. 4(a), a significant reduction of $|\nabla T_i|$ occurs, albeit with some time delay (i.e., the reduction in $|\nabla T_i|$ is not simultaneous with the γ_E reduction). Anti-correlation between $\langle \delta T_i^2 \rangle$ at $r = r_2$ and $\langle \delta V_{||}^2 \rangle$ at $r = r_4$ and the increase of γ_{ZF} at $r = r_3$ during the PVGI excitation indicate that this time delay is due to turbulence suppression by nonlocal interactions among fluctuations.

In conclusion, PVGI can be excited in ITB plasmas with strong flow shear and plays a significant role in ITB dynamics. The significant change of Reynolds stress observed in power ramp simulations[12] originates from the excitation of PVGI. Parallel momentum is redistributed following the Reynolds stress change driven by PVGI. During this redistribution, the radial profile of $\nabla V_{||}$ changes dramatically near the q_{min} position, affecting the $E \times B$ shear at ITB. Forward transition occurs during $\nabla V_{||}$ relaxation, induced by the PVGI. The Reynolds stress burst caused by the PVGI can induce outward momentum transfer and leads to the back transition. We also show that stronger fluctuations outside the ITB induced by PVGI can suppress weaker fluctuations inside the ITB, via zonal flow induction. A similar nonlocal effect is also observed in the barrier back-transition. As mentioned earlier, the main drawback of the present numerical model is that it retains only resonant modes. In contrast, non-resonant modes have maximal intensities at the q_{min} position, due to their minimal Landau damping. Thus, the intensity gradient, which is a major symmetry breaker,[10] will be reduced near the ITB, once nonresonant modes are included. In this regard, our results are susceptible to overestimation of the Reynolds stress and intrinsic rotation. In actual ITB experiments, however, external torque is usually applied and could play a synergistic role with intrinsic torque to generate a large shear flow. In this case, the effects of non-resonant modes may not qualitatively change our findings, since PVGI will be excited if the rotation shear is sufficiently large.

The authors are grateful to Dr. X. Garbet for providing the TRB code. This work was supported by the World Class Institute (WCI) Program of the National Research Foundation of Korea (NRF) funded by the Ministry of Education, Science and Technology of Korea (MEST) (NRF Grant No. 2009-001) and by the U.S. Department of Energy under Grant No. DE-FG02-04ER54738.

[1]P. C. deVries *et al.*, Nucl. Fusion **49**, 075007 (2009).
[2]M. E. Austin *et al.*, Bull. Am. Phys. Soc. **52**, UP8.00059 (2007).
[3]P. A. Politzer *et al.*, Nucl. Fusion **48**, 075001 (2008).
[4]P. Mantica *et al.*, Phys. Rev. Lett. **107**, 135004 (2011).
[5]E. G. Highcock *et al.*, Phys. Rev. Lett. **105**, 215003 (2010).
[6]H. Jhang *et al.*, Phys. Plasmas **19**, 042302 (2012).
[7]T. W. Versloot *et al.*, Nucl. Fusion **51**, 103033 (2011).
[8]X. Litaudon, Plasma Phys. Controlled Fusion **48**, A1 (2006).
[9]Ö. D. Gürcan *et al.*, Phys. Plasmas **14**, 042306 (2007).
[10]Ö. D. Gürcan *et al.*, Phys. Plasmas **17**, 112309 (2010).
[11]C. L. Fiore *et al.*, Nucl. Fusion **50**, 064008 (2010).
[12]S. S. Kim *et al.*, Nucl. Fusion **51**, 073021 (2011).
[13]P. J. Catto *et al.*, Phys. Fluids **16**, 1719 (1973).
[14]N. Mattor and P. H. Diamond, Phys. Fluids **31**, 1180 (1988).
[15]S. L. Newton *et al.*, Plasma Phys. Controlled Fusion **52**, 125001 (2010).
[16]A. G. Peeters *et al.*, Phys. Plasmas **12**, 072515 (2005).
[17]X. Garbet *et al.*, Phys. Plasmas **9**, 3893 (2002).
[18]K. Itoh *et al.*, J. Plasma Fusion Res. SERIES **8**, 119 (2009).
[19]X. Garbet *et al.*, Phys. Plasmas **8**, 2793 (2001).
[20]A simulation keeping power flat for a while before bring it down that is more akin to experiments was also performed. The ITB was sustained during flat-top phase and basic features during transitions did not change.
[21]J. Candy *et al.*, Phys. Plasmas **11**, 1879 (2004).
[22]H. Biglari *et al.*, Phys. Fluids B **2**, 1 (1990).
[23]K. H. Burrell *et al.*, Phys. Plasmas **4**, 1499 (1997).